Composite Grid Atomistic Continuum Method: An adaptive approach to bridge continuum with atomistic analysis

D.K. Datta[1], R.C. Picu[1] and M.S. Shephard[1]
[1]Scientific Computation Research Center, RPI, Troy, NY 12180-3590

Abstract

The Composite Grid Atomistic Continuum Method (CACM), a method to couple continuum and atomistic models is proposed in a three dimensional setting. In this method, atomistic analysis is used only at places where it is needed in order to capture the intrinsically non-linear/non-local behavior of the material at the atomic scale, while continuum analysis is used elsewhere for efficiency. The atomistic model is defined on a separate grid that overlaps the continuum in selected regions. The atomistic and the smallest scale continuum model are connected by appropriately defined operators. The continuum model provides boundary conditions to the discrete model while the atomistic model returns correcting eigenstrains. The adaptive selection of the spatial regions where the atomistic correction is needed is made based on error indicators developed to capture the non-linearity and non-locality modeling errors. The method is applied to represent dislocation nucleation from crack tips and nanoindentation in aluminum.

1 Introduction

The macroscopic scale behavior of a material is governed by processes that occur on finer length and time scales. Therefore, accurate representation of larger scale behavior requires capturing the multiphysics behavior on multiple intermediate scales, from the atomic to the system level.

This endeavor faces several barriers. The macro-scale deformation which is typically represented by continuum models, is usually incompatible with the deformation modes of a discrete system. The interactions at the atomic scale are defined by interatomic potentials, functions that express the energy of an atom in terms of the local system structure. All material properties follow from the potential used. At the atomic scale the mechanical behavior is non-linear and intrinsically non-local. Non-linear continuum models are used on a regular basis and non-local models may be defined and used in the continuum sense [1]. However, the calibration of these higher order continuum models on the lattice response is not always straightforward or possible [2]. This complexity can be avoided by directly using discrete models over portions of the domain where the lower order constitutive models are not acceptable [3]-[4].

One of the important features of discrete models which is difficult to be captured by continuum models stems from the non-convexity of the potential of the system of atoms. This function has a complicated shape in the 3N dimensional space, where N is the number of atoms in the system. The potential surface has numerous minima which renders the solution of the discrete model non-unique. An example is the recovery of the geometry and energy of the lattice after a dislocation swipes across the model. By contrast, the energy of the continuum is usually a convex function of the degrees of freedom of the model with a unique minimum.

Fully fine scale modeling of deformation processes is not practical because of the massive computational resources that would be required. An alternative is to perform fine scale modeling only where needed, at those places where the continuum does not represent the mechanical behavior properly, for instance, close to dislocation cores, at crack tips, surfaces and interfaces, etc. The enhancement of the continuum solution with information from underlying discrete models may be performed by using embedded and sequential schemes. In sequential schemes, the gross output

(statistical averages) of a scale is input into the upper scale, while in embedded schemes, the various scales are coupled explicitly in a single multiscale model.

The most used methods to couple discrete and continuum models are sequential. An example from this class is the calibration of various continuum model parameters, such as stiffness, diffusion coefficient, thermal conductivity, etc, based on the discrete model response determined in separate discrete simulations [5]. Another example is the calibration of crystal plasticity phenomenological rules based on discrete dislocation dynamics simulations [6]. Various representative volume element-based techniques belong to this class. In these methods, the constitutive behavior of the continuum is defined by the response of an underlying discrete simulation performed with the boundary conditions imposed by the continuum. This method is similar to the multiscale continuum models commonly used to represent the behavior of heterogeneous materials [7]. However, the definition of a representative volume element (RVE) may be difficult in some situations, while prescribing boundary conditions for the RVE is often ambiguous.

The embedded schemes relieve some of these difficulties. In embedded schemes, the system is represented as a whole, with both continuum and discrete models being used simultaneously. The discrete model is used at sites where higher accuracy is desired or where the continuum is unable to capture the actual physics. This type of coupling removes the ambiguity regarding the boundary conditions to be used for the discrete model, as they are naturally derived from the continuum coarser scale. All methods belonging to this category face the problem of matching the two scales in the transition zone where the finer scale meets (or overlaps) the coarse scale. In the transition zone it is usually required that the discretization on the coarse grid is refined down to the atomic scale [3], [8]-[10]. Another drawback of these methods is that the continuum is not simply connected, as "cuts" are introduced in those zones where a discrete model is used. This limitation is important if adaptivity is sought (see [4], [9]-[10] and the references therein).

To optimize the simulation process it is essential that the atomistic analysis is used only at the places where required for accuracy of the solution while, at the same time, the atomistic region remains as small as possible for efficiency. This requires the development of adaptive methods based on error indicators to automatically select the sites and size of the atomistic regions within the domain [4].

A new method, the Composite Grid Atomistic Continuum Method, is proposed here to couple the atomistic analysis with the continuum analysis in a 3-dimensional setting. In this method atomistic regions are overlaid on the continuum region at the places of high field gradients or where the non-linear and non-local behavior of the lattice is important. Since this method uses an overlaid grid, it eases the difficulty of matching atomistic and continuum grids and the implementation of an adaptive procedure. This method can be generalized to a multiscale environment in which the discrete scales are coupled with multiple continuum scales. In the current implementation the continuum is discretized using finite elements. The necessity of correcting the solution by including a discrete grid is determined based on appropriate error indicators. In these regions a discrete model is used on a finer grid with the discrete and smallest scale continuum grids connected using appropriate operators. The discrete grid receives displacement boundary conditions from the continuum grid and returns corrective eigenstrains. The adaptive selection of the spatial regions where the atomistic correction is needed is made based on error indicators developed to detect modeling errors.

In the next Section the Composite Grid Atomistic Continuum Method is described. In Section 3 numerical examples that illustrate the method are presented. The method is then extended to an adaptive setting in Section 4. The modeling error indicators on which the adaptivity is based are described in Section 4 and the adaptive algorithm for automated selection of the atomisitic region within the domain is presented. In Section 5 numerical examples that demonstrate the adaptivity

capability are discussed.

2 The methodology

A general methodology for coupling atomic and continuum levels based on an embedded scheme is introduced in this section. In the proposed method the system of interest is subdivided into various levels which are embedded into each other as shown in Figure 1. In general the levels may have different models and/or levels of discretization. A fine scale model or the same model with a finer resolution is used while going down the cycle therefore enriching the representation. To link two successive levels, a proper linking operator has to be designed. The operator linking a coarse level with a fine level is referred to as the Coarse To Fine Scale linking operator (C2F), while the operator performing the reverse operation is referred to as the Fine To Coarse Scale linking operator (F2C).

In Composite Grid Atomistic Continuum Method the finer level is overlapped on the coarser level only at places where the finer level is required. This approach has the following advantages:

(a) *Accuracy*: The finer scale improves the accuracy of the obtained solution.

(b) *Overlaid grids*: This approach removes the requirement of matching refinement levels on the coarse and fine grids. Furthermore, the coarse grid does not need to be artificially made multiply connected in order to include the finer model (no "cut-out" is necessary). This leads to more effective applications of adaptive modifications of the grids at various levels.

(c) *Not completely a new setting*: This method has the advantage of utilizing already developed and well established procedures for solving the atomistic and continuum level problems, respectively. The new method integrates these procedures in a modular code.

In this work the focus is on linking continuum and discrete models. Linking all other continuum levels that represent larger scales may be performed using various available techniques, e.g. [11]. In the following sub-sections, the general setting is introduced followed by the description of the Composite Grid Atomistic Continuum Method, and the definition of the operators used. For the present discussion it is assumed that the lattice is in equilibrium, at zero Kelvin. Since the atomic vibrations are not included in the model, only the spatial scale linking between the continuum and discrete levels is performed. Atomic vibrations (finite temperatures) may be included in the model in a statistical sense as in [12], with no significant modifications to the basic procedure described below (Section 6).

2.1 The setting

Let the system consist of multiple spatial levels with the finer levels occupying smaller domains then the coarser levels, such that, $G_0 < G_1 < ... < G_{l-1} < G_l < ...$, as shown in Figure 1, where G_l denotes the grid at level l with $l = 0$ corresponding to the finest model, i.e. $G_0 = A$. The objective is to solve the problem at level $l = l_{max}$. The solution at the highest level l_{max} depends on the solution at a lower level $l_{max} - 1$, which in turn depends on the solution at $l_{max} - 2$, and so forth. Hence, to reach the desired solution, all the lower levels $l < l_{max}$ must be linked.

To connect the different levels $l = 0, 1, 2...$, while going down from the coarse to the fine level, the Coarse To Fine Scale linking (C2F) operator is defined as follows,

$$P_{G_l G_{l-1}} : G_l \rightarrow G_{l-1} \quad \text{for } l = 1, 2, ..., l_{max} \tag{1}$$

The C2F operator is a mapping from the coarse grid G_l into the fine grid G_{l-1}.

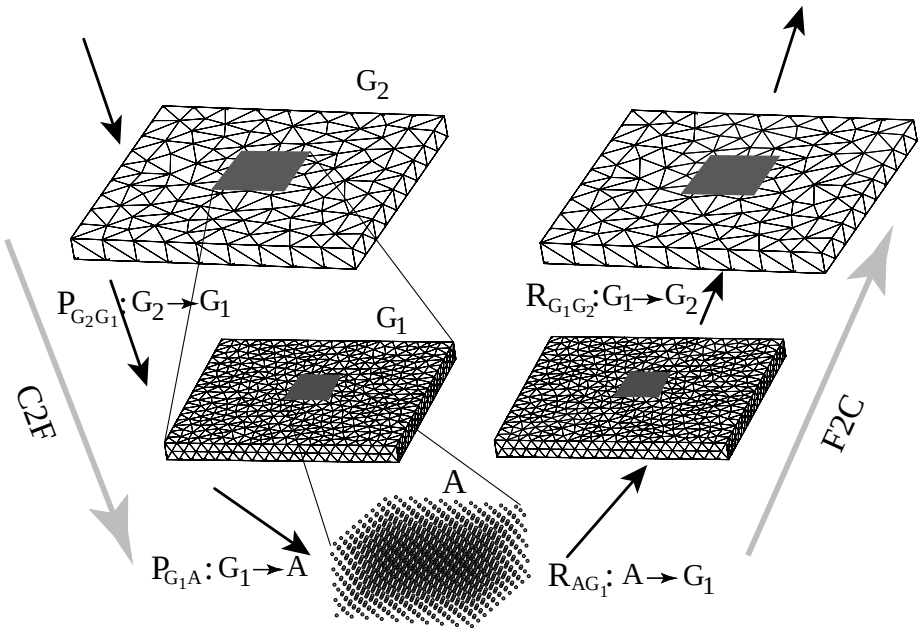

Figure 1: A schematic diagram of the composite grid setting.

The Fine To Coarse Scale linking (F2C) operator which maps the fine grid G_{l-1} functions into the coarse grid G_l functions is described as:

$$R_{G_{l-1}G_l} : G_{l-1} \rightarrow G_l \quad \text{for } l = 1, 2, ..., l_{max} \tag{2}$$

To link two successive levels, the C2F and the F2C operators needs to be defined.

2.2 The Composite Grid Atomistic Continuum Method (CACM)

In this section the two operators, C2F and F2C, that link the smallest scale continuum level with the atomistic level are given, followed by a description of the continuum and the atomistic models considered. Let G_1 denote the continuum level of interest and $A \equiv G_0$ denote the atomistic level, as shown in Figure 2.

Let $u_i^{G_1}$ be the solution of the problem on the continuum grid G_1, which is the actual domain of interest, and u_i^A be the solution on the underlying atomistic grid A. The atomistic grid is overlaid in regions, e.g. at the crack tip, where the continuum model does not accurately represent the solution of the actual problem of interest. Let Ω_I be the region occupied by a cluster of atoms $\mathcal{C}_I$ which is refered to as the *interior atoms*, Ω_B be the region surrounding Ω_I, and let $\mathcal{C}_B$ be the cluster of atoms in Ω_B which is refered to as the *pad atoms* as shown in Figure 2. Ω'_I, and Ω'_B is the region of grid B where Ω_I, and Ω_B of grid A overlaps the continuum grid. The C2F operator for the proposed method CACM which maps the continuum level G_1 solution to the atomistic level A is then defined as:

$$(P_{G_1A}\ u_i^{G_1})(\mathbf{x}) \stackrel{\text{def}}{=} u_i^{G_1}(\mathbf{x}) \quad \forall \mathbf{x} \in \Omega_B \tag{3}$$

$u_i^{G_1}(\mathbf{x})$ is the displacement field obtained from the solution at the level G_1. This operation sets up the boundary condition based on the continuum solution for the atomistic analysis by prescribing the displacement for the pad atoms $\mathcal{C}_B$. In the case where the solution at the continuum level is obtained using the pth order finite element method, the operator used here is the pth order

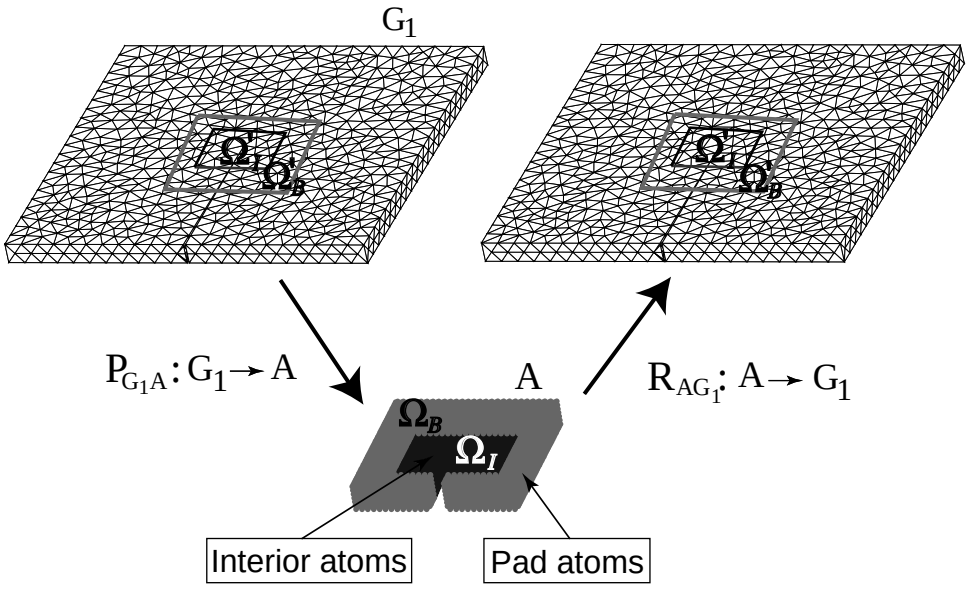

Figure 2: A schematic diagram of the linking of continuum with the atomistic grid.

piecewise interpolation over the finite element(s) containing point $\mathbf{x}$. The F2C operator for CACM maps the atomic level A solution to the continuum level G_1, and is defined as

$$(R_{AG_1}\ u_i^A)(\mathbf{x}) \stackrel{\text{def}}{=} \tilde{u}_i^A(\mathbf{x}) \quad \forall \mathbf{x} \in \Omega_I' \tag{4}$$

where $\tilde{u}_i^A$ is the displacement field obtained by post-processing the displacements $u_i^{A,p}(\mathbf{x}_p)$ of the atoms. This sets up the correction of the continuum solution in region Ω_I'. Since the solution at the atomistic level is discrete, i.e. the displacements obtained from the atomistic solution are defined only at the locations of the atoms, a continuous representation $\tilde{u}_i^A(\mathbf{x})$ of the field is created by post-processing the displacements of the atoms.

In the present implementation the post-processing is performed using a weighted average scheme. Let R_c be the cut-off radius of the interatomic potential, and $\mathcal{C}_{R_c}$ be the cluster of atoms within the distance R_c from the point $\mathbf{x}$ where the displacement is computed. The post-processed displacement $\tilde{u}_i^A(\mathbf{x})$ at point $\mathbf{x}$ within region Ω_I' is then given by

$$\tilde{u}_i^A(\mathbf{x}) = \frac{\sum\limits_{p \in \mathcal{C}_{R_c}} u_i^{A,p}(\mathbf{x}_p)\ w(r_p)}{\sum\limits_{p \in \mathcal{C}_{R_c}} w(r_p)} \quad \forall \mathbf{x} \in \Omega_I' \tag{5}$$

where $w(r_p)$ is a weighting function defined by

$$w(r_p) = 1 - 3\Big(\frac{r_p}{R_c}\Big)^2 + 2\Big(\frac{r_p}{R_c}\Big)^3 \tag{6}$$

with r_p being the distance between point $\mathbf{x}$ and the position $\mathbf{x}_p$ of an atom p. Various other post-processing schemes may be used, such as interpolation, least-squares fitting etc. Such operators may be found in the literature related to data fitting through a large set of scattered data points (see [13]-[14] and the references therein).

For the purpose of illustration of the proposed method, an anisotropic linear elasticity model was used for the continuum. This model is solved using the finite elment method. The discrete model is represented in the atomistic sense using an interatomic potential. The details of the two models are discussed next.

The continuum model: Let the governing equations for the continuum model be

$$-\sigma_{ij,j} = f_i \ \text{ in } \ \mathrm{G}_1 \tag{7}$$

where $\sigma_{ij} = C_{ijkl}\ \epsilon_{kl}$ are the components of the stress tensor; $\epsilon_{kl} = (u^{G_1}_{k,l} + u^{G_1}_{l,k})/2$ are the components of the strain tensor (small deformations), and C_{ijkl} is the stiffness tensor. With prescribed displacements $\bar{u}_i$ on Γ_D, and tractions g_i prescribed on Γ_N

$$u^{G_1}_i = \bar{u}_i \ \text{ on } \ \Gamma_{\mathrm{D}}, \quad \sigma_{\mathrm{ij}}\mathrm{n_j} = \mathrm{g_i} \ \text{ on } \ \Gamma_{\mathrm{N}} \tag{8}$$

The variational formulation of (7)-(8) is given by

Find $u^{G_1}_i \in H^1_D(G_1) \stackrel{\text{def}}{=} \left\{ v_i \in H^1(G_1) \middle| v_i = 0 \ \text{ on } \ \Gamma_{\mathrm{D}} \right\}$ such that

$$\mathcal{B}(u^{G_1}_i, v_i) = \mathcal{L}(v_i) \quad \forall v_i \in H^1_D(G_1) \tag{9}$$

where

$$\mathcal{B}(u^{G_1}_i, v_i) = \int_{G_1} v_{(j,k)} C_{jklm} u_{(l,m)}\ dG_1 \tag{10}$$

is the bilinear form and $v_{(j,k)} = (v_{j,k} + v_{k,j})/2$, and

$$\mathcal{L}(v_j) = \int_{G_1} v_j f_i\ dG_1 \ + \ \int_{\Gamma_N} v_j g_i\ d\Gamma_N, \tag{11}$$

is the linear form.

Let $u^{G_1,FE}_i$ be the finite element solution of $u^{G_1}_i$ obtained by solving the following discrete variational problem:

Find $u^{G_1,FE}_i \in \mathcal{U}^{h,p}(\Omega) \subset H^1_D(\Omega)$ such that

$$\mathcal{B}(u^{G_1,FE}_i, v_i) = \mathcal{L}(v_i) \quad \forall v_i \in \mathcal{U}^{h,p}(G_1) \tag{12}$$

Here $\mathcal{U}^{h,p}(G_1) \subset H^1_D(G_1)$ is the space of the finite element functions spanned by piecewise polynomials of degree p defined over a spatial discretization of G_1 by conforming finite elements. Details of the variational formulation and its finite element approximation are given in [15].

Remark: The selection of the method used for the solution of the continuum level is independent of the proposed CACM.

The atomistic model: Let

$$\Pi(\mathbf{x}_1, \mathbf{x}_2, ..., \mathbf{x}_N) = \sum_{p \in \mathcal{C}_I} \Pi_p \quad \forall\ p \in \mathcal{C}_I \tag{13}$$

be the total energy of all N atoms in the discrete region(s), with Π_p being the energy of atom p. $\mathbf{x}_p$ denotes the atomic positions. Solving the discrete model reduces to finding the minimum of

the internal energy (13) with respect to the position of the atoms (the degrees of freedom of the discrete system),

$$\Pi_{min} = \min_{\mathbf{x}_1,\mathbf{x}_2,...,\mathbf{x}_N} \Pi(\mathbf{x}_1, \mathbf{x}_2, ..., \mathbf{x}_N) \tag{14}$$

with the condition

$$u_i^{A,q}(\mathbf{x}_q) = \bar{u}_i^q(\mathbf{x}_q) \quad \forall q \in \mathcal{C}_B \tag{15}$$

where $u_i^{A,q}(\mathbf{x}_q)$ denotes the displacement of atom q, and $\bar{u}_i^q(\mathbf{x}_q)$ is the prescibed displacement of atom $q \in \mathcal{C}_B$ at position $\mathbf{x}_q$.

Remark: The selection of the method to solve the atomistic problem is independent of the proposed CACM. The minimum energy configuration may be found, for instance, by molecular statics (functional minimization) or by a Monte Carlo procedure [16].

Based on the description of the continuum model, the atomistic model and the operators, the algorithm for the Composite Grid Atomistic Continuum Method is stated as follows:

Step 1. Solve the continuum model problem (12) on G_1.

Step 2. $P_{G_1A} : G_1 \rightarrow A$ (C2F: Sets up the boundary condition for the atomistic analysis)

Step 3. Solve the atomistic model problem (14)-(15) on A with the condition

$$\bar{u}_i^q(\mathbf{x}_q) = u_i^{G_1,FE}(\mathbf{x}_q) \quad \forall q \in \mathcal{C}_B \tag{16}$$

Step 4. $R_{AG_1} : A \rightarrow G_1$ (F2C: Sets up the correction of the continuum solution)

Step 5. Re-solve the continuum model problem (12) on G_1 with the additional condition

$$u_i^{G_1} = \tilde{u}_i^A \quad \text{on} \quad \Omega_{\mathrm{I}}' \tag{17}$$

Hence, in CACM, the continuum model is solved first, then the C2F operator sets the displacement boundary condition for the atomistic analysis (i.e the displacement for the pads atoms) based on the continuum level solution. The atomistic model is then solved, and its solution is imposed through the F2C operation as a correction to the continuum in region Ω_I', i.e where the interior atoms overlaps the continuum region. The continuum is solved again with the corrective eigenstrains imposed.

Remark: It is noted that in the proposed method, rather than minimizing a single functional for the coupled scale system [3]-[4], the solution at each level is obtained separately with meaningful boundary conditions derived from the other level. This alternative is selected for efficiency. The small scale model is intrinsically non-linear. In regions where fields and their gradients are small, a linearized approximation is usually considered satisfactory. By solving the two problems separately, the non-linearity of the small scales does not pollute the whole problem allowing for an efficient solution of the large scale problem. The uniqueness of the global solution is insured by the scale linking operators. Similar ideas are used in other numerical schemes (see [17]-[19] and references therein).

3 Numerical examples for CACM

In this section two numerical examples are presented in order to demonstrate the coupling of the continuum with the atomistic model using CACM. The computations are performed in a 3D setting, however, for the purpose of illustration and verification, the problems chosen are self-similar in loading and geometry in one of the directions and therefore 2D-like.

The material considered in these examples is aluminium. The elastic constants for aluminium are $\bar{C}_{11} = 1.181Mbar$, $\bar{C}_{12} = 0.623Mbar$, and $\bar{C}_{44} = 0.367Mbar$ in the principal crystallographic axes. All symmetries of the cubic crystal apply. $\bar{C}_{pq}$ are the elastic constants C_{ijkl} written in the reduced indicial notation taking into account of the symmetries of C_{ijkl} [15].

An embedded-atom potential is used to represent the energetics of the material in the atomistic region. The total internal energy of all the atoms $p \in \mathcal{C}_I$ is given by

$$\Pi(\mathbf{x}_1, \mathbf{x}_2, ..., \mathbf{x}_N) = \sum_{p \in \mathcal{C}_I} \Pi_p(r_{pq}), \qquad \Pi_p(r_{pq}) \stackrel{\text{def}}{=} U_p(\rho_p) + \Phi_p(r_{pq}) \tag{18}$$

where

r_{pq} is the distance between atoms p with position vector $\mathbf{r}_p$ and q with position vector $\mathbf{r}_q$

$$r_{pq} \stackrel{\text{def}}{=} |\mathbf{r}_p - \mathbf{r}_q| \tag{19}$$

ρ_p is the electron density at atom p

U_p is the embedding energy representing the interaction of atom $p \in \mathcal{C}_I$ with the electron cloud of density $\rho_p(r_{pq})$,

$\Phi_p(r_{pq})$ is the pair interaction energy for atoms p and q

$\Phi_p(r_{pq})$ is modelled as a pairwise interaction over all nuclei

$$\Phi_p(r_{pq}) = \frac{1}{2} \sum_{\substack{q \in \mathcal{C}_{R_c} \\ q \neq p}} \phi_{pq}(r_{pq}) \tag{20}$$

where p are the interior atoms, and q are the atoms within the cut-off radius from the position of atom p, ϕ_{pq} is a pairwise interaction potential between atoms p, and q. The electron density at atom p is approximated as the superposition of the electron densities due to the surrounding atoms at the location of p

$$\rho_p = \sum_{\substack{q \in \mathcal{C}_{R_c} \\ q \neq p}} f_q(r_{pq}) \tag{21}$$

where f_q is the electron density generated by atom q at a distance r_{pq}. The embedded atom potential used here was developed by Ercolessi and Adams [20] by fitting to a large database of *ab-initio* interatomic forces and measured material properties. Note that the width of the pad region should be at least twice the cut-off radius R_c of the potential in order to provide a complete set of neighbors for the atoms in $\mathcal{C}_I$.

The minimization of the total internal energy with respect to the positions of atoms, $\mathbf{x}_1, \mathbf{x}_2, ..., \mathbf{x}_N$, is performed using a conjugate gradient minimizer from the Harwell library [21].

Example 3.1: Figure 3a shows an aluminium block under uniaxial tensile load discretized using finite elements and overlaid with an atomic grid in the middle. Figure 3b shows the plot of the

displacement in the loading direction obtained using continuum analysis, and the coupled analysis. It also shows the solution for the case where the coupling is deliberately blocked. The atomic region in the middle of the block acts as a rigid body in the case when there is no information transfer between the continuum and atomistic levels and the displacement in that region is zero. On the other hand, when the coupling is effective, the solution obtained by CACM closely matches the linear elasticity solution.

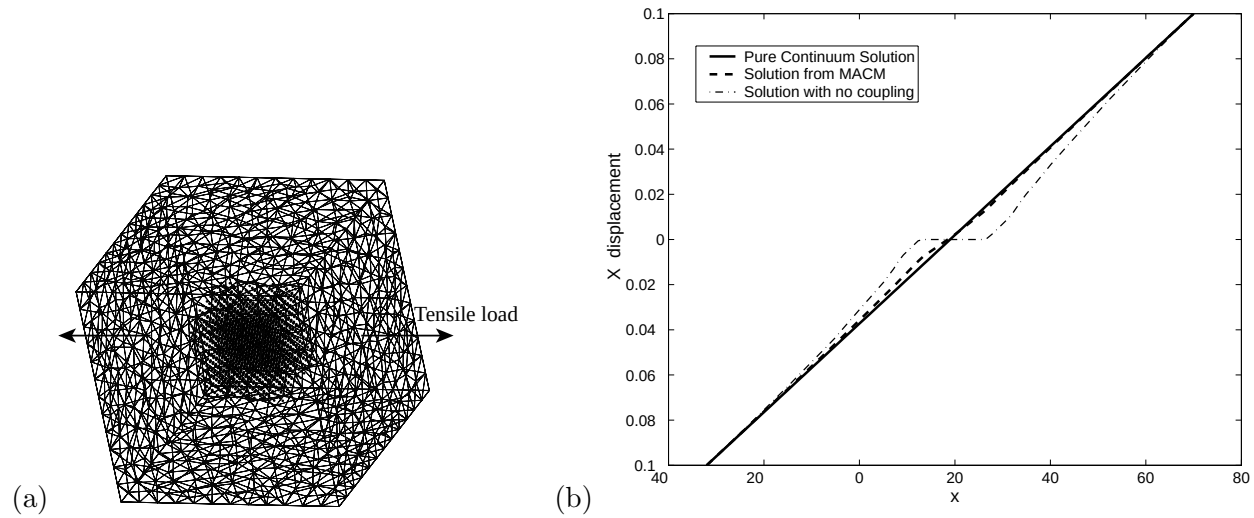

Figure 3: (a) An overlaid grid of finite elements and atoms to model a block of aluminium cube under tensile load. (b) Plots of solutions of the continuum analysis, the coupled analysis using CACM, and the case in which there is no coupling between the two models.

Example 3.2: Figure 4a shows an aluminum plate containing a crack discretized using finite elements and overlaid with an atomistic grid at the crack tip. The crystallographic orientation is shown in Figure 4a. The crack orientation is selected to favor dislocation nucleation from the tip rather than brittle crack propagation. The Mode I crack solution

$$u_1 = K\sqrt{\frac{r}{2\pi}}\,\cos\left(\frac{\theta}{2}\right)\left(k-1+2\sin^2\left(\frac{\theta}{2}\right)\right) \qquad u_2 = K\sqrt{\frac{r}{2\pi}}\,\sin\left(\frac{\theta}{2}\right)\left(k+1-2\cos^2\left(\frac{\theta}{2}\right)\right) \tag{22}$$

where $k = 3 - 4\nu$, ν being the Poisson ratio, was imposed as displacement boundary condition for the continuum problem,

$$u_1^{G_1} = u_1, \qquad u_2^{G_1} = u_2 \qquad \text{on } \Gamma_{\mathrm{D}}. \tag{23}$$

K is the ratio of stress-intensity factor and shear modulus. The plate is loaded by incrementally increasing K. Figures 4b and c show the zoomed-in view of the atomistic region near the crack tip as obtained with CACM for the steps corresponding to $K = 1.0\sqrt{\text{Å}}$, and $K = 1.5\sqrt{\text{Å}}$, respectively. In Figure 4b, dislocations are seen to nucleate from the tip and glide along their glide planes, as expected. This solution is compared with that obtained from a fully atomistic model of size four times larger than that of the atomistic grid in Figure 4. The same Mode I crack solution was imposed as the boundary condition for the fully atomistic simulation

$$u_1^{A,q}(\mathbf{x}_q) = u_1, \quad u_2^{A,q}(\mathbf{x}_q) = u_2 \;\; \forall q \in \mathcal{C}_B \tag{24}$$

Figures 4d and e show the atomic configuration obtained from this model at the same spatial region near the crack as in Figures 4b and c and corresponding to the same load increment. The

comparison of the two sets of data shows that the results obtained using CACM and from the fully atomistic simulation are similar. Defects nucleate from the tip at the same load level ($K = 1.0\sqrt{\text{Å}}$) and propagate in a similar manner, which demonstrates the effectiveness of the coupling.

In this simulation, for testing and visualization purposes, the model is kept thin and periodic boundary conditions are used in the direction along the crack tip. Therefore, the dislocations nucleating from the tip are forced to have straight dislocation lines parallel to the crack tip. This leads to an anomaly in the dislocation pattern forming in front of the tip: Lomer locks are created by the reaction of the trailing partials of two edge dislocations moving on radial glide planes away from the tip. This structure is sessile and, due to the symmetry of the field, would not move or break as the stress increases. At higher levels of stress, other dislocations moving in the backward direction nucleate. It is expected that if the model size increases in the third direction, dislocation loops would nucleate from the tip allowing for the formation of a realistic defect structure.

4 Adaptive CACM (ACACM)

To optimize the method it is essential that the atomistic analysis is used only at those places where required for accuracy of the solution. At the same time the atomistic region should remain as small as possible for efficiency. The location and the size of the atomistic region must change during a simulation as defects nucleate and propagate. It is essential to automate the process of selecting the sites and size of the atomistic region(s) within the domain. In this section an adaptive version of the CACM (ACACM) is described. The adaptive process is driven by error indicators designed to capture the modeling error introduced by the use of the continuum model. These indicators control the size of the atomistic region.
The modeling error indicators reflect the following three characteristics of the solution:

(a) *Non linearity* ($\eta_{Non-Lin}$): The non-linearity error originates from the fact that the material behavior of the discrete system in the elastic domain is intrinsically non-linear, while linear elasticity is used as the constitutive model for the continuum. The error is related to the magnitude of the strain. The indicator used here is based on comparing the first order (quadratic) term in the strain energy expansion with the higher order terms of the expansion.
Let $\mathcal{E}$ be the strain energy, which is expanded in series with respect to the strains ϵ_{ij} as

$$\mathcal{E} = C'_{ij}\ \epsilon_{ij}\ +\ \frac{1}{2}\ C''_{ijkl}\ \epsilon_{kl}\ \epsilon_{ij}\ +\ \frac{1}{6}\ C'''_{ijklmn}\ \epsilon_{mn}\ \epsilon_{kl}\ \epsilon_{ij}\ +\ O(\epsilon^4) \tag{25}$$

where C'_{ij}, $C''_{ijkl} \equiv C_{ijkl}$, and C'''_{ijklmn} are the zeroth, first, and second order elastic constants. By definition, for the continuum $C'_{ij} \equiv 0$, which represents the condition of vanishing stress in a undeformed perfect lattice. Neglecting the third and higher order terms, the error in strain energy due to the consideration of the first order term only is given by

$$e = \mathcal{E} - \frac{1}{2}\ C_{ijkl}\ \epsilon_{kl}\ \epsilon_{ij} = \frac{1}{6}\ C'''_{ijklmn}\ \epsilon_{mn}\ \epsilon_{kl}\ \epsilon_{ij}\ + O(\epsilon^4) \tag{26}$$

and the relative error can then be written as

$$e_{REL} \approx \frac{\frac{1}{6}\ C'''_{ijklmn}\ \epsilon_{mn}\ \epsilon_{kl}\ \epsilon_{ij}}{\mathcal{E}} \tag{27}$$

Since the exact strain energy $\mathcal{E}$ is not known it is approximated by

$$\mathcal{E} \approx \frac{1}{2}\ C_{ijkl}\ \epsilon_{kl}\ \epsilon_{ij}\ +\ \frac{1}{6}\ C'''_{ijklmn}\ \epsilon_{mn}\ \epsilon_{kl}\ \epsilon_{ij} \tag{28}$$

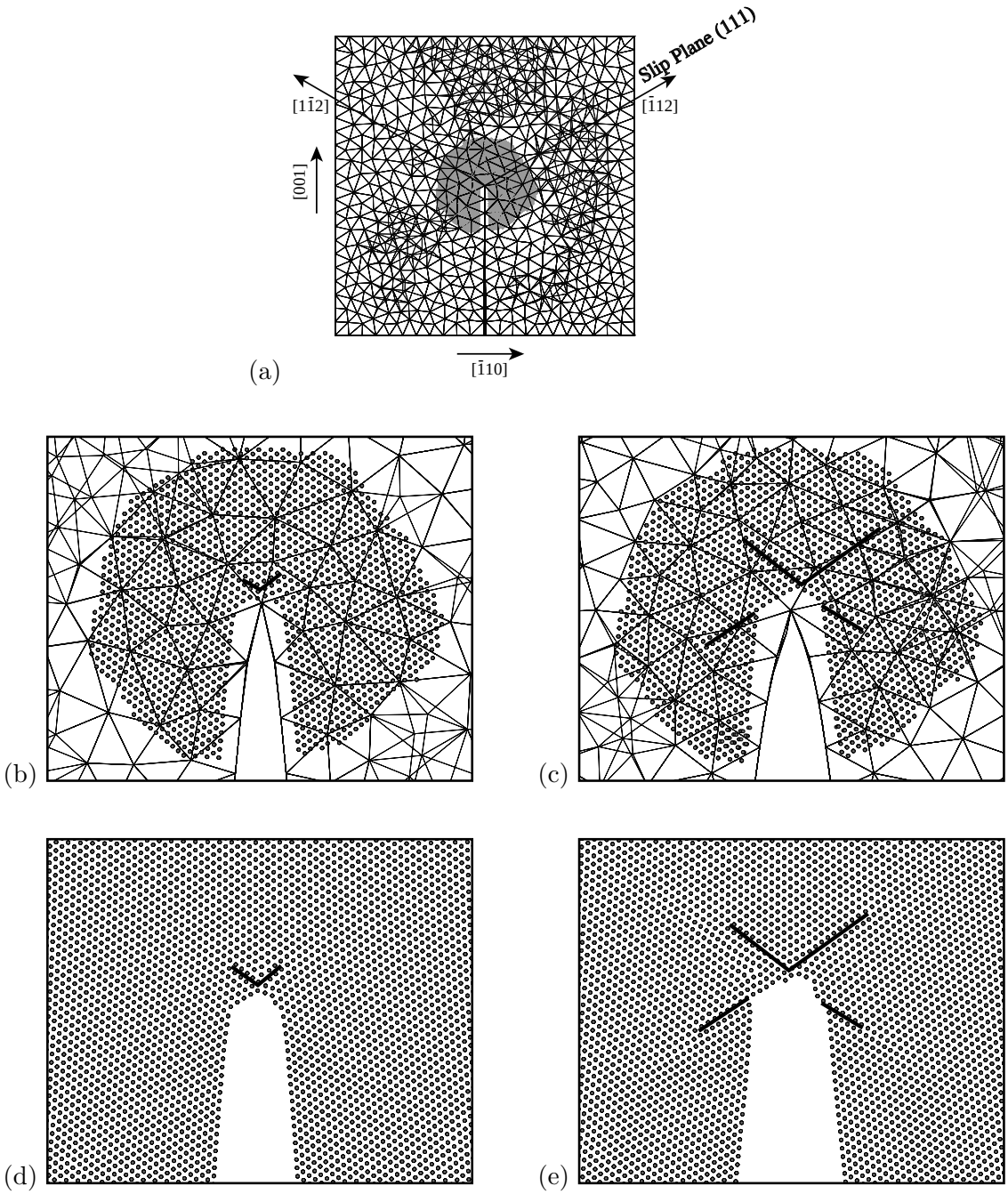

Figure 4: (a) An overlaid grid of finite elements and atomistic region at the crack tip modeling a plate with a crack. The atomistic region near the crack tip for the results of coupled analysis using CACM corresponding to load steps (b) $K = 1.0\sqrt{\text{Å}}$, and (c) $K = 1.5\sqrt{\text{Å}}$. (d) and (e) show corresponding results obtained from a fully atomistic analysis of the same problem. The atomistic region considered for this case is four times the size of the atomistic region (shown in a) used for the simulation using CACM. The thick black lines indicate dislocation that nucleated from the tip. The outer ends of the lines indicate the current position of the respective defect.

with which the non-linearity error indicator over a sub-domain τ is defined as

$$\eta_{Non-Lin} = \sqrt{\frac{\int \left(\frac{1}{6}\ C'''_{ijklmn}\ \epsilon_{mn}\ \epsilon_{kl}\ \epsilon_{ij}\right)^2\ d\tau}{\int \left(\frac{1}{2}\ C_{ijkl}\ \epsilon_{kl}\ \epsilon_{ij}\ +\ \frac{1}{6}\ C'''_{ijklmn}\ \epsilon_{mn}\ \epsilon_{kl}\ \epsilon_{ij}\right)^2\ d\tau}} \tag{29}$$

The higher order elastic constants used in the error indicator are determined such that they are compatible with the potential used. To this end, a series of separate atomistic simulations are performed in which a block of atoms is deformed homogeneously uniaxially and multiaxially. The stresses derived from (25) is fitted (first 3 terms only) to the stress-strain curves obtained from these separate atomistic simulations.

The second order constants that need to be determined for a cubic lattice are [22]:

$$\begin{aligned}
\bar{C}'''_{111} = \bar{C}'''_{111} = \bar{C}'''_{111} &= a_1 \\
\bar{C}'''_{112} = \bar{C}'''_{113} = \bar{C}'''_{122} = \bar{C}'''_{223} = \bar{C}'''_{133} = \bar{C}'''_{233} &= a_2 \\
\bar{C}'''_{123} &= a_3 \\
\bar{C}'''_{144} = \bar{C}'''_{255} = \bar{C}'''_{366} &= a_4 \\
\bar{C}'''_{155} = \bar{C}'''_{166} = \bar{C}'''_{244} = \bar{C}'''_{266} = \bar{C}'''_{344} = \bar{C}'''_{355} &= a_5 \\
\bar{C}'''_{456} &= a_6
\end{aligned} \tag{30}$$

where $\bar{C}'''_{pqr}$ are the elastic constants C'''_{ijklmn} written in the reduced index notation. To evaluate the constant $\bar{C}'''_{111}$, for example, the lattice is deformed by imposing a strain ϵ_{11} and the stress is computed using the virial formula [5] and based on the potential employed for the atomistic analysis. Since all other strains are zero, the stress σ_{11} is given by

$$\sigma_{11} = \bar{C}_{11}\ \epsilon_{11} + 1/2\ \bar{C}'''_{111}\ \epsilon_{11}^2 \tag{31}$$

which provides an equation for $\bar{C}'''_{111}$. The other second order constants may be determined in a similar manner by applying different strain states.

(b) *Non locality* ($\eta_{Non-Loc}$): Stress production in the lattice is intrinsically non-local. The stress tensor at the location of an atom (e.g. computed using the virial formula) depends on the position (and displacement) of neighboring atoms located at some distance from the representative atom. Therefore, the stress at the location of that atom is determined by the strain in a spherical neighborhood of it of radius R_c. On the other hand, the continuum constitutive description is, in most cases, local. The stress at a point depends on the strain at that point only. Although non-local constitutive formulations may be used in the continuum which, if calibrated based on the atomistic response, would eliminate in part this error, they add a computational burden that may not be always worthy of consideration. In the present formulation in which the simplest possible model is selected for the continuum, the non-local nature of the stress in the discrete region leads to a discrepancy with respect to the continuum which must be corrected.

If the stress field has no gradients, the non-local stress becomes equal to the local one. The non-locality error is important only where the field varies significantly on a length scale comparable with R_c. Such situations are encountered, for example, close to crystal defect cores, at interfaces and crack tips.

A constant stress field corresponds to a displacement field with zero second derivatives. For the purpose of evaluating the non-local influence, one could consider estimates of the local

second derivatives or consider the difference in the first derivatives of the displacement field over the local length scale, R_c as an approximation to the second derivative. Although this appears to be a reasonable straightforward process, there is an inherent assumption that the displacement field being examined is sufficiently smooth. Since the finite element field is only C_0 between elements, the first derivatives have finite jumps and the second derivatives are undefined on element boundaries.

There are a number of alternatives available to increase the order of continuity of the displacement fields or evaluate specific order derivatives of the displacements. A number of procedures have been developed to determine C_0 derivative fields (see [23] for a summary of several of them). One such procedure that has been found highly effective in discretization error estimation is the patch recovery technique [24]. Methods to calculate estimates of the second derivatives have been developed and range from variational-based methods [25] to Green's identity-based methods [26].

Since the patch recovery technique is already being used as part of the adaptive mesh discretization error control process, a first estimate of the influence of non-locality is based on looking how much the recovered C_0 derivative fields vary over the length scale associated with R_c.

One of the main objectives of the present method is to avoid mesh refinement in the continuum down to the scale of the interatomic spacing. Therefore, the field gradients where the continuum mesh is used must be small enough such that the fields do not vary over the volume of an element more than a certain threshold. If the same tolerance is used as in the non-locality error indicator, the mesh discretization criterion supersedes the non-locality criterion. Hence, assuming that the mesh is not fully refined it is sufficient to use just the mesh discretization criterion to determine the non-locality. A similar non-locality error indicator was used in [4].

(c) *Non-convexity* ($\eta_{Non-Con}$): The energy of the lattice is a non-convex function in the 3N dimensional space of the degrees of freedom of all N atoms in the system. Therefore, stable lattice equilibrium may be reached in numerous configurations. The most frequently encountered non-convexity problem in lattices is associated with the motion of atoms (displacements) by multiples of the lattice spacing. In such cases, the energy of the discrete system does not change. A continuum model on the other hand, would lead in general to a non-zero strain energy density for a non-vanishing displacement field. In embedded methods in which the discrete and continuum descriptions are used simultaneously, the continuum needs to be informed about this discrepancy and its strain energy should be brought in agreement with that of the discrete system.

An example in which such correction is needed is the recovery of the lattice (structure and energy) after a dislocation glides by along a glide plane. If the dislocation motion were represented in the continuum sense, this operation would leave behind a narrow region of thickness equal to the interplanar distance d in which a large strain energy corresponding to a residual shear strain of magnitude b/d is stored (b is the Burgers vector). Specialized indicators are needed to instruct the continuum model to treat such deformation as an eigenstrain. In the examples discussed in this article the defects that nucleate from stress concentration sites do not leave the discrete region and therefore, the correction for non-convexity is not required. This indicator is currently being developed and will be reported in an upcoming article.

Let $\Lambda_{Non-Lin}$ denote the region where the non-linearity error is higher than a user defined tolerance $Tol_{Non-Lin}$:

$$\eta_{Non-Lin} > Tol_{Non-Lin} \tag{32}$$

and $\Lambda_{Non-Loc}$, and $\Lambda_{Non-Con}$ denote the regions where

$$\eta_{Non-Loc} > Tol_{Non-Loc} \quad \text{and} \quad \eta_{Non-Con} > Tol_{Non-Con} \tag{33}$$

where $Tol_{Non-Loc}$, and $Tol_{Non-Con}$ are user defined tolerances for the non-locality and non-convexity criterion. The atomistic region Ω_I is then determined as the union of the three domains:

$$\Omega_I = \Lambda_{Non-Lin} \cup \Lambda_{Non-Loc} \cup \Lambda_{Non-Con} \tag{34}$$

Remark: When the continuum model is solved using the finite element method, the indicators are computed for each finite element. Hence, the sub-domains τ in (29) are the volumes of the finite elements. In that case $\Lambda_{Non-Lin}$, $\Lambda_{Non-Loc}$, and $\Lambda_{Non-Con}$ denote groups of finite elements for which (32) and (33) are fulfilled.

Based on the CACM and the error indicators described above the Adaptive Composite Grid Atomistic Continuum Method (ACACM) which automates the process of determining the atomistic region within the continuum can then be described as follows:

Step 1. Solve the continuum model problem on G_1.

Step 2: Compute the indicators $\eta_{Non-Lin}$, $\eta_{Non-Loc}$, and $\eta_{Non-Con}$ for all the elements in the mesh. Determine the atomistic region Ω_I based on (32)-(34).

Step 3. $P_{G_1A} : G_1 \rightarrow A$

Step 4. Solve the atomistic model problem

Step 5. $R_{AG_1} : A \rightarrow G_1$

Step 6. Resolve the continuum model problem on G_1

5 Numerical examples for ACACM

In this section numerical examples are given to demonstrate the adaptive version of the proposed method. As in the case discussed in Section 3, aluminium is the material of choice for these examples. The simulations are performed in a 3-dimensional setting, but the problem has a 2D character.

Example 5.1: A setting similar to that in Example 3.2 is considered here. However, in this case the location and size of the atomistic region are not pre-defined, rather are selected adaptively. At the beginning of the simulation, the model is purely continuum. As the crack is loaded, large strains and field gradients appear at the crack tip. The model is adaptively updated by overlaying an atomistic region at locations determined by the error indicators. The indicators are computed in each finite element based on the continuum field quantities. As stated above, the non-convexity error indicator is not used in these simulations.

Figures 5a, b and c show the deformed continuum model and atomistic grid at several load increments defined by $K = 0.2, 1.4$, and $2.0\ \sqrt{\text{Å}}$, respectively. Figures 5d, e and f show the enlarged view of the atomistic region at the crack tip. The size of the discrete region is small at small loads and increases with increasing K. Note that the characteristic dimension of the continuum mesh is much larger than the interatomic distance. The discrete region in Figure 5a is mandated by the

large strains and strain gradients at the crack tip. In Figure 5b and c, the nucleation of dislocations from the crack tip as well as a more intense crack tip field require a larger discrete region. The discrete region extends in the direction in which dislocations move on their respective glide planes, as expected. Dislocation nucleation is observed at exactly the same value of $K = 1.0\sqrt{\text{Å}}$, as in Example 3.2 and in the purely atomistic larger scale simulation.

Example 5.2: The simulation of a nano-indentation process is considered next. The model consists of a block of Al indented by a rigid indenter. The effect of the indenter is imposed as a displacement boundary condition on the body. The crystallographic orientation of the sample is chosen such to favor dislocation nucleation from the stress concentration sites at the corners of the indenter. The <111> direction is horizontal in the figures, while the indentation direction is <110>.

Figure 6 shows the model at various stages of indentation. The atomistic region is adaptively overlayed on the continuum. Figure 6a, b, and c correspond to 1.0, 8.0 and 15.0 Å indentation depth, respectively. The displacement in the indentation direction is uniform across the indenter front. Figures 6e, f and g show the magnified views of the atomistic region corresponding to each step. As the indenter is pushed in, edge dislocations nucleate from the edges of the indenter, as expected in this geometric configuration. The defects propagate into the material and the adaptive procedure extends the atomistic region accordingly. At large indentation levels, incipient twinning is observed right under the indenter.

The adaptive procedure overlays the atomistic region on the continuum only where needed and reduces the computational cost compared to a fully atomistic simulation. In Example 5.1, in the adaptive simulation, the initial model had only 2996 degrees of freedom, which increased as the atomistic region grew in size due to the nucleation of dislocations as the simulation progressed (14710 dofs for $K = 1.0\sqrt{\text{Å}}$, 115242 for $K = 2.6\sqrt{\text{Å}}$). If the adaptive procedure is not used, a fully discrete model for the entire domain (shown in Figure 5a) have to be used for every step of the simulation even though a fully discrete representation of the entire domain is not required at every step. A fully discrete model of the entire domain shown in Figure 5a has 216750 degrees of freedom. Since the atomistic model is non-linear, this dramatically increase the computational cost. For example, the fully atomistic simulation in Example 3.2 was 12 times computationally more expensive than the simulation performed using ACACM in Example 5.1.

6 Summary and conclusions

A composite grid method for coupling atomistic and continuum models was presented. The continuum is represented by finite elements, while the atomistic problem is solved by lattice statics. The discrete region overlays the continuum in regions where higher accuracy is needed. Operators to couple the two levels were defined. The coarse to fine scale operator transfers the continuum displacement to the discrete grid and imposes the boundary conditions for the solution of the atomistic problem. The fine to coarse operator returns corrective eigenstrains to the continuum. The solution is searched over two separate phase spaces, one corresponding to the discrete and one to the continuum problem, and uniqueness of the solution is insured by the scale linking operators and the iterative procedure. The method was shown to provide results similar with those obtained from large scale purely atomistic simulations of the same problem.

An adaptive version of the method was developed in which the size and location of the discrete region are selected based on error indicators. These correct the non-linearity error, associated with the magnitude of the strains, and the non-locality error, associated with the magnitude of the strain gradients. A further error indicator correcting the non-convexity error is defined without

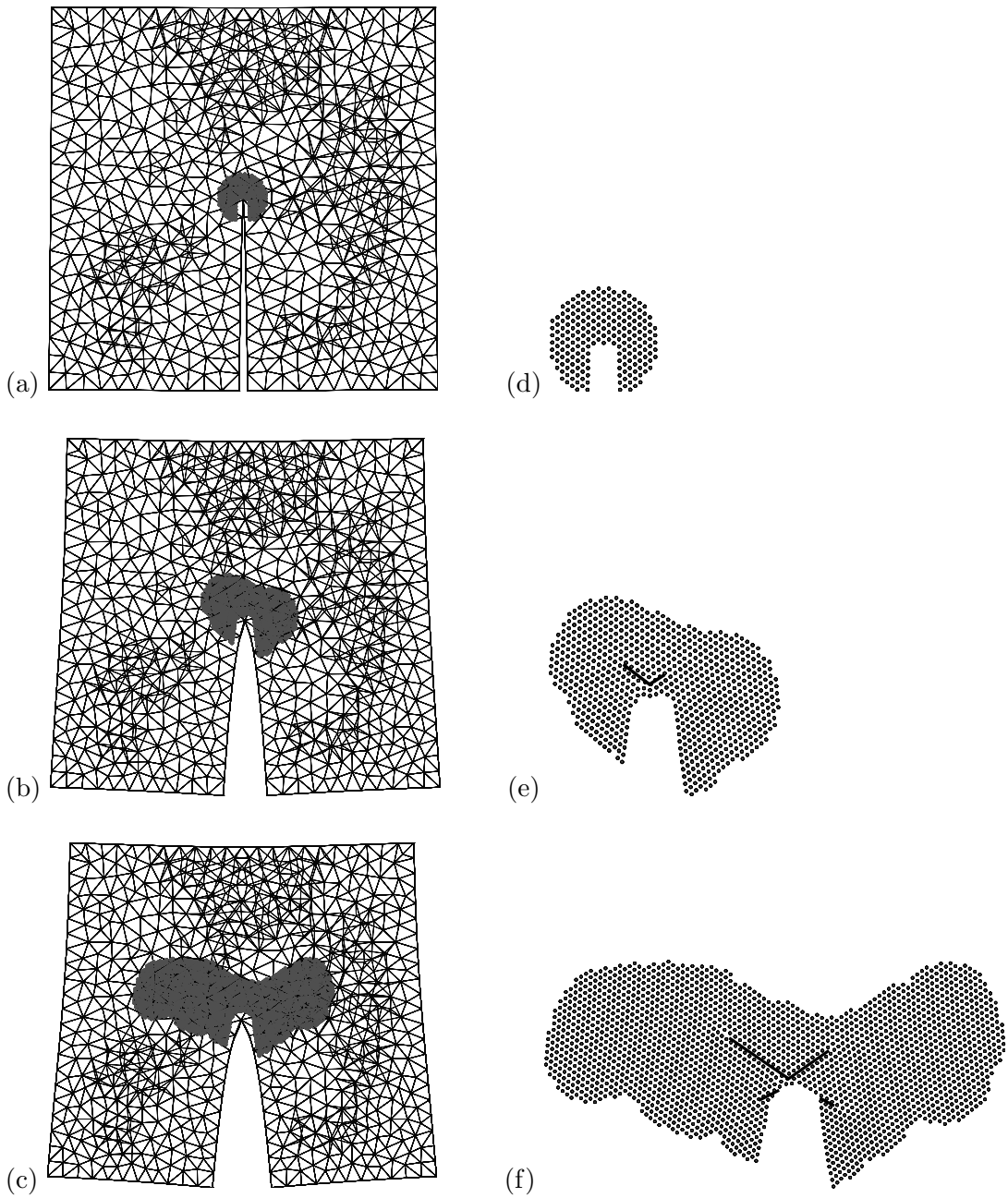

Figure 5: Adaptive model of a Mode I crack tip region for load steps characterized by (a) $K = 0.2\sqrt{\text{Å}}$, (b) $K = 1.4\sqrt{\text{Å}}$, (c) $K = 2.0\sqrt{\text{Å}}$. The size and location of the discrete region is defined by the error indicators. (d), (e) and (f) show the magnified view of the corresponding atomistic region for the three load steps. The thick black lines indicate dislocations nucleating from the tip and moving in the respective glide plane.

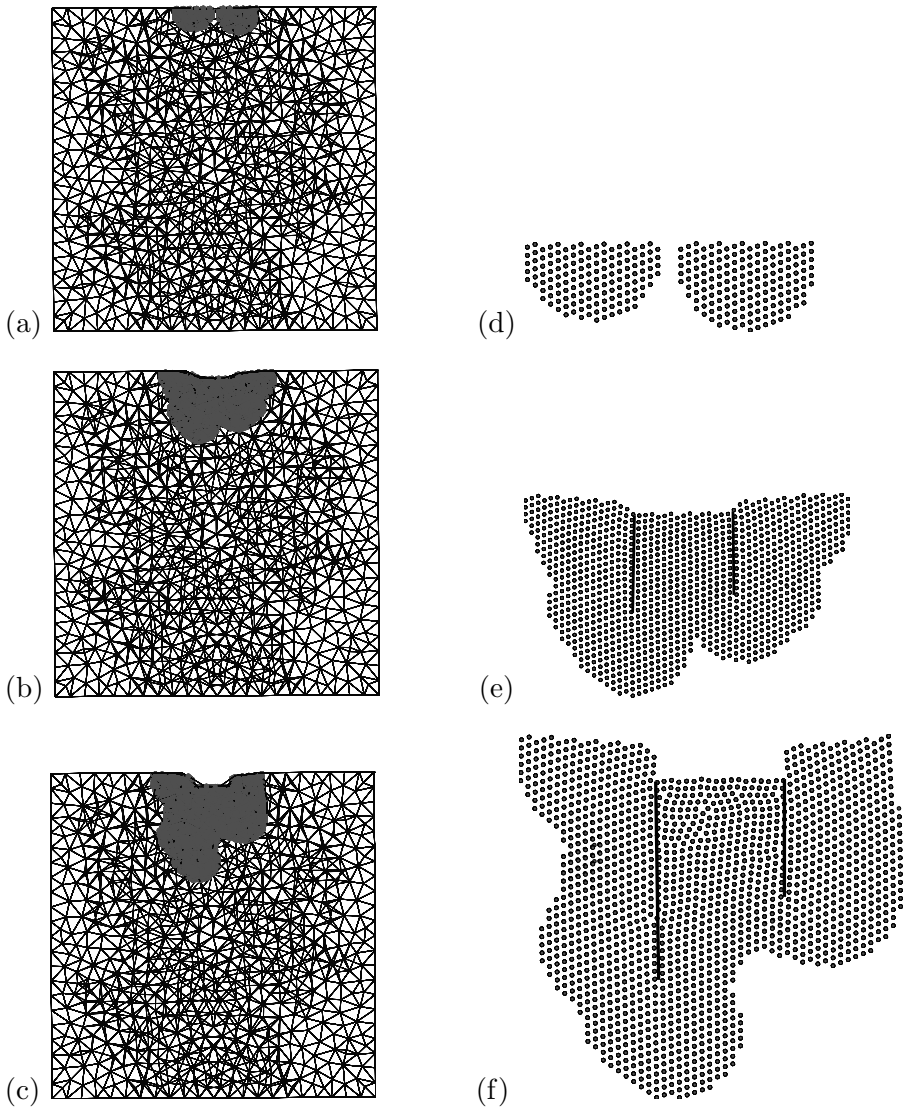

Figure 6: Adaptive model of the nano-indentation of a block of Al. (a), (b) and (c) show the structure below the indented and the size and location of the discrete region for indetation displacements of 1.0, 8.0 and 15.0 Å respectively. (d), (e) and (f) show the magnified view of the corresponding atomistic region for the three load steps. The thick black lines indicate dislocation nucleation.

being used in the examples discussed. The adaptive method was applied to the analysis of defect nucleation from a crack tip and that of nanoindentation with substantial reductions of the number of degree of freedom required.

The advantages of the present method are: the atomistic model is used where needed to correct the continuum solution therefore improving its accuracy, the procedure is adaptive, the discrete grid is an overlay to the continuum model which eliminates the need of cuts being made in the continuum in order to accommodate the atomistic patch, the continuum mesh does need to be refined down to the interatomic length scale, and the implementation makes use of existing established techniques for solving the continuum and the atomistic regions and allows for their integration in a self-consistent framework.

The current method and implementation allow for lattice statics calculations only, corresponding to a temperature of 0K, represent only a single physical phenomenon, i.e. the deformation field, and are still to be proved on the simulation of a large number of defects and discrete regions evolving simultaneously. Work on extending the method to finite temperatures and to multiple physical phenomena as well as on considering fully 3D large scale models is underway.

References

[1] A.C. Eringen, "Screw dislocation in non-local elasticity", *J. Phys.*, (10) 671-678, 1977.

[2] R.C. Picu, "On the functional form of non-local elasticity kernels", *J. Mech. Phys. Sol.* (50) 1923-1939, 2002.

[3] F.F. Abraham, J. Broughton, N. Bernstein, and E. Kaxiras, "Spanning the length scales in dynamic simulation", *Comput. Phys.*, (12) 538-546, 1998.

[4] V.B. Shenoy, R. Miller, E.B. Tadmor, D. Rodney, R. Phillips, and M. Ortiz, "An adaptive finite element approach to atomic scale mechanics-the quasicontinuum method", *J. of Mech. and Phys. of Solids*, (47) 611-642, 1999.

[5] J.M. Haile, *Molecular dynamics simulations: elementary methods*, Wiley, New York, 19 92.

[6] H.M. Zbib, M. Rhee, and J.P. Hirth, "On plastic deformation and the dynamics of 3D dislocations", *Int. J. Mech. Sci.* (40) 113-126, 1998.

[7] J. Fish, and K. Shek, "Finite deformation plasticity for composite structures: computational models and adaptive strategies", *Comp. Meth. Appl. Mech. Eng.*, (172) 145-174, 1999.

[8] S. Kohlhoff, S. Schmauder, "A New Method for Coupled Elastic-Atomistic Modelling", Atomistic Simulation of Mater-ials: Beyond Pair Potentials", *Eds.: V. Vitek, D.J. Srolovitz, Plenum Press, New York, London*, 411-418, 1989.

[9] S. Kohloff, P. Gumbsch, and H.F. Fischmeister, "Crack propagation in b.c.c. crystals studied with a combined finite element and atomistic model", *Phil. Mag. A*, (64) 851-878, 1991.

[10] R.E. Miller, "Direct coupling of atomistic and continuum mechanics in computational materials science", *Int. J. Multiscale Comput. Eng.*, (1) 57-72, 2003.

[11] W. Hackbusch, *Multigrid methods and applications*, Springer-Verlag, Berlin, 1985.

[12] R. LeSar, R. Najafabadi and D.J. Srolovitz, "Finite temperature defect properties from free energy minimization", *Phys. Rev. Lett.* (63) 624-627, 1989.

[13] Michael S. Floater, Armin Iske, "Multistep scattered data interpolation using compactly supported radial basis functions", *Journal of Computational and Applied Mathematics* (73) 65-78, 1996.

[14] Robert J. Renka, "Multivariate Interpolation of Large Sets of Scattered Data", *ACM Transactions on Mathematical Software* (14) 139-148, 1988.

[15] T.J.R. Hughes, *The finite element method - Linear static and dynamic finite element analysis*, Dover Publications, New York, 2000.

[16] K. Binder, and D.W. Heermann, *Monte Carlo simulation in statistical physics: an introduction*, Springer-Verlag, Berlin, 1992.

[17] Jean-David Benamou, and Bruno Despres, "A domain decomposition method for the helmholtz equation and related optimal control problems", *J. of Comp. Phy.*, (136) 68-82, 1997.

[18] Barry F. Smith, Petter E. Bjørstad, and William Gropp, *Domain Decomposition: Parallel Multilevel Methods for Elliptic Partial Differential Equations*, Cambridge University Press, 1996.

[19] C. Felippa, K. C. Park and C. Farhat, "Partitioned Analysis of Coupled Mechanical Systems", *Computer Methods in Applied Mechanics and Engineering*, (190) 3247-3270, 2001.

[20] F. Ercolessi, J. Adams, "Interatomic potentials from 1st principles calculations - the force matching method", *Europhysics Letters*, (26) 583-588, 1993.

[21] HSL. Harwell Subroutine Library. A Catalogue of Subroutines. (*www.cse.clrc.ac.uk/nag/hsl*)

[22] C. Teodosiu, *Elastic models of crystal defects*, Springer-Verlag, Berlin, 1982.

[23] P.P. Silvester, and D. Omeragic, "Comparative experimental study of differentiation methods on finite elements" , *Int. J. Applied Electromagnetics in Materials*, (4) 123-136, 1993.

[24] O.C. Zienkiewicz, and J.Z. Zhu, "Superconvergent patch recovery and a posteriori error estimates. Part 1 : the recovery technique, Part 2: error estimates and adaptivity", *Int. J. for Num. Meth. in Eng.*, (30) 1331-1382, 1992.

[25] J.F. Remacle, X. Li, M.S. Shephard, and J.E. Flaherty, "Anisotropic Adaptive Simulation of Transient Flows", submitted to *Int. J. for Num. Meth. in Eng.*, 2003.

[26] D. Omeragic, and P.P. Silvester, "Differentiation of finite element solutions to non-linear problems", *Int. J. Num. Modeling: Electronic Networks, Devices and Fields*, (13) 305-319, 2000.